Phosphatidylglucoside Exists as a Single Molecular Species with Saturated Fatty Acyl Chains in Developing Astroglial Membranes†

Yasuko Nagatsuka,‡ Yasuhiro Horibata,‡ Yasuhiro Yamazaki,§ Masami Kinoshita,‡ Yoko Shinoda,‡ Tsutomu Hashikawa,§ Hiroyuki Koshino,|| Takemichi Nakamura,⊥ and Yoshio Hirabayashi*,‡,#

Hirabayashi Research Unit, Neuronal Circuit Mechanisms Research Group, and Laboratory for Neuronal Architecture, RIKEN Brain Science Institute, Wako, Saitama 351-0198, Japan, Molecular Characterization Team and Biomolecular Characterization Team, RIKEN, Wako, Saitama 351-0198, Japan, and Core Research for Evolutional Science and Technology (CREST) of Japan Science and Technology Agency (JST), Kawaguchi, Saitama 332-0012, Japan

Received April 4, 2006; Revised Manuscript Received May 24, 2006

ABSTRACT: We previously found that phosphatidylglucoside (PtdGlc), a novel glycolipid expressed in HL60 cells, plays a role in forming signaling microdomains involved in cellular differentiation. Because cells contain minute levels of PtdGlc, pure PtdGlc is very difficult to isolate. Thus, its complete structure has never been assessed. To aid in analyzing PtdGlc, we generated a PtdGlc-specific monoclonal antibody, DIM21, by immunizing mice with detergent-insoluble membranes isolated from HL60 cells [Yamazaki, Y., et al. (2006) *J. Immunol. Methods 311*, 106−116]. DIM21 immunostaining of murine CNS tissues revealed stage- and cell type-specific localization of the DIM21 antigen during development, with especially high levels of expression in radial glia/astroglia. DIM21 immunostained cultured hippocampal astroglia in a punctate fashion. To characterize the structure of PtdGlc, we isolated DIM21 antigen from fetal brains. Using successive column chromatography, we purified two previously unrecognized glycolipids, PGX-1 and PGX-2, from embryonic day 21 rat brains. DIM21 reacted more strongly to PGX-2 than to PGX-1. Structural analyses with 600 MHz ^{1}H NMR, FT-ICR mass spectrometry, and GC revealed that PGX-1 is phosphatidyl β-D-(6-*O*-acetyl)glucopyranoside and PGX-2 is phosphatidyl β-D-glucopyranoside. The yields of PGX-1 and PGX-2 were approximately 250 ± 150 and 440 ± 270 nmol/g of dried brains, respectively. Surprisingly, both glycolipids were composed exclusively of C18:0 at the C1 position and C20:0 at the C2 position of the glycerol backbone. This saturated fatty acyl chain composition comprising a single molecular species rarely occurs in known mammalian lipids and provides a molecular basis for why PtdGlc resides in raftlike lipid microdomains.

In all vertebrate cells, most glycosphingolipids (GSLs)[1] are localized within the outer leaflet of the plasma membrane. Recent studies show that GSLs form microdomains or lipid rafts by clustering cholesterol, glycosylphosphatidylinositol (GPI)-anchored proteins, and acylated proteins (*1*−*5*). GSLs in microdomains have multiple functions, acting as receptors for toxins (*6*, *7*), participating in cell adhesion (*8*−*10*), modulating cell growth (*11*, *12*), and initiating signal transduction (*13*, *14*). In the central nervous system (CNS), lipid microdomains also play various roles, acting as nonreceptor neuronal Src signaling platforms (*15*), mediating chemotropic axonal guidance in nerve growth cones (*9*, *16*), acting as neuron−glia interaction platforms (*17*, *18*), and acting as sites where amyloid precursors accumulate (*19*).

Using an anti-carbohydrate "i" monoclonal antibody, we first detected in human cord red blood cells a phosphoglycerolipid containing glucose as its sole sugar (*20*). Interestingly, we also found that HL60 cells, a promyelocytic leukemia cell line, also possess a similar phospholipid, termed phosphatidylglucoside (PtdGlc). This lipid localizes to a detergent-insoluble membrane (DIM) fraction (*21*). We found that rGL-7, a recombinant Fab fragment of anti-i, elevates the level of PtdGlc in the DIM fraction derived from HL60 cells. The complete structure of PtdGlc remains to be elucidated, because HL60 cells contain minute PtdGlc levels, levels too low for successful isolation and purification of the PtdGlc required for detailed structural analysis.

† This work was supported by Grant-in-Aid 12140201 (Scientific Research on Priority Areas [B]) to Y. Hirabayashi, the RIKEN President Discretionary Fund (to Y. Hirabayashi), and the Core Research for Evolutional Science and Technology (CREST) of Japan Science and Technology Agency (JST) (to Y. Hirabayashi).

* To whom correspondence should be addressed: Hirabayashi Research Unit, Neuronal Circuit Mechanisms Research Group, RIKEN Brain Science Institute, Wako, Saitama 351-0198, Japan. Telephone and fax: +81-48-467-6372. E-mail: hirabaya@riken.jp or ynaga@brain.riken.jp.

‡ Hirabayashi Research Unit, Neuronal Circuit Mechanisms Research Group, RIKEN Brain Science Institute.

§ Laboratory for Neuronal Architecture, RIKEN Brain Science Institute.

|| Molecular Characterization Team, RIKEN.

⊥ Biomolecular Characterization Team, RIKEN.

Core Research for Evolutional Science and Technology (CREST) of Japan Science and Technology Agency (JST).

[1] Abbreviations: GSL, glycosphingolipid; mAb, monoclonal antibody; FT-ICR-MS, Fourier transform ion cyclotron resonance mass spectrometry; SORI-CID, sustained off-resonance irradiation/collision-induced dissociation; TOCSY, total correlation spectroscopy; HMBC, heteronuclear multiple-bond coherence spectra; GC, gas chromatography; Glc, glucose; PtdGlc, phosphatidyl β-D-glucopyranoside; PI/PtdIns, phosphatidylinositol; PGly, phosphatidylglycerol; DIM, detergent-insoluble membrane.

10.1021/bi0606546 CCC: $33.50
Published on Web 06/27/2006

Katagiri et al. (*22*, *23*) reported that the DIM fraction acts as an effective immunogen. Indeed, we successfully prepared many monoclonal antibodies (mAbs) to DIM by immunizing mice with a DIM fraction isolated from rGL-7-stimulated HL60 cells. We found that one of these mAbs, DIM21, preferentially reacts with PtdGlc in HL60 cells (*24*). Using this antibody, we detected DIM21 antigen in the murine CNS and found that its expression was developmentally regulated. This observation suggested that PtdGlc might exist in the nervous system. Here we report the isolation of DIM21-immunoreactive lipid antigen from fetal rat brains and describe the complete structural analysis of this antigen by gas chromatography (GC), 600 MHz NMR, and FT-ICR mass spectrometry. We also describe the chemical structure of another novel glycolipid, acylated PtdGlc, a form of PtdGlc acetylated at C6 of its glucose ring.

MATERIALS AND METHODS

Monoclonal Antibody. Monoclonal antibody DIM21 was generated by immunizing the DIM fraction isolated from rGL-7-stimulated HL60 cells as described by Yamazaki et al. (*24*). DIM21-producing cells were cultured in RPMI-1640 medium supplemented with 10% fetal calf serum, 100 μg/mL streptomycin, and 100 units/mL penicillin at 37 °C in a 5% CO_2 humidified atmosphere. For antibody preparation, the cells were transferred into SFM-101 (Nissui Pharmaceutical Co., Ltd.) at a density of 2×10^6 cells/mL and then cultured for 2 weeks. After the culture media had been harvested, IgM was precipitated to 50% saturation with ammonium sulfate for 1−2 weeks at 4 °C, then dissolved in Tris-buffered saline, dialyzed against the same buffer, and purified by using an immunoassist MGPP gel (Kanto Chemical Co., Inc.), according to the supplier's recommendations.

Immunohistochemical Staining. A pregnant female rat with embryonic day 21 (E21) fetuses was deeply anesthetized, and fetuses were isolated. The fetuses were then transcardially perfused with 4% paraformaldehyde in a 0.1 M phosphate buffer solution, and brains were carefully removed, embedded in agarose blocks, and then cut into 50 μm thick sections using a vibrating microtome (VT1000S; Leica).

Free-floating sections were used for immunohistochemistry. After blocking with 10% normal goat serum in PBS, we incubated the sections with 10 μg/mL mAb DIM21 overnight at 4 °C and washed them with PBS (2×5 min and 1×15 min), and the bound antibody was visualized with Alexafluor 488-conjugated anti-mouse IgM secondary antibody (2 μg/mL; Molecular Probes Inc., Carlsbad, CA). After being washed thoroughly with PBS, sections were mounted onto glass slides with IMMUMOUNT (Thermo Shandon, Milford, MA) and observed with a confocal laser microscope (model FV1000, Olympus, Tokyo, Japan).

Hippocampal Cell Culture. Primary cultures of dissociated hippocampal neural cells were prepared from fetal Wistar rats (SLC, Shizuoka, Japan) at E19, as described previously (*25*) using a D-MEM/F12 (1:1) medium without cytosine β-D-arabinoside.

Isolation of PtdGlc. Ten pregnant Wistar rats with embryonic day 21 (E21) fetuses were deeply anesthetized, and brains of the fetuses were removed immediately, placed into liquid nitrogen, and then lyophilized. Total lipids were extracted from the lyophilized brains (approximately 2.0 g dry weight) using 100 mL of chloroform and methanol (C:M at 2:1, v/v) twice and then with C:M and water (W) (5:8:3, v/v/v) twice using a Polytron aggregate homogenizer (Kinematica AG, Littau-Lucerne, Switzerland). The latter extraction solvent containing water was essential for efficient extraction of PtdGlc. After evaporation, the lipid extract was treated with 0.5 unit of phosphatidylinositol (PtdIns)-specific phospholipase C[2] (PIPLC; Sigma-Aldrich Inc., St. Louis, MO) at 37 °C overnight to remove PtdIns (*26*). The reaction mixture was subjected to Folch's partition, and then the organic layer was applied to a phenyl boronate−agarose column (PBA-60; Millipore, Billerica, MA) (*21*, *27*, *28*) to enrich the glycolipids, including PtdGlc. PBA-unbound lipids (PB-1) were washed out with 5 column volumes of C:M (9:1, v/v), and then the PBA-bound fraction (PB-2) was eluted with 5 column volumes of C:M:W (5:5:1, v/v/v). After evaporation, the PB-2 fraction was applied to a Q-Sepharose column [activated with 1 M sodium acetate in M:W (1:1, v/v)], washed with methanol, and pre-equilibrated with C:M:W (30:60:8, v/v/v). After the samples had been washed with the starting solvent for 10 min, the lipids retained in the column were eluted with gradient solutions, starting with C:M:W (30:60:8, v/v/v) and ending with C:M and aqueous 0.25 M sodium acetate (30:60:8, v/v/v), for 90 min. Lipids (mainly gangliosides) remaining in the column were then washed out with C:M and aqueous 2 M sodium acetate (30:60:8, v/v/v). The elution profile of lipids was monitored by TLC and TLC immunostaining with DIM21 according to the method of Higashi et al. (*27*, *28*).

PtdGlc-containing fractions were pooled and partitioned with Folch's solvent system, and then the organic solvent layer was dried using an evaporator, dissolved in 1 mL of C:M (2:1, v/v), and then applied to an Aquasil Senshu Pack column (Senshu Scientific Co., Tokyo, Japan) for HPLC. After the samples had been washed with C:M (9:1, v/v), elution was carried out with gradient solutions, starting with C:M (9:1, v/v) and ending with C:M (7:3, v/v), for 90 min. PtdGlc was identified by TLC and TLC immunostaining using DIM21 (*27*, *28*). The amount of PtdGlc was calculated according to phosphorus content, which was determined by treating the 70% perchloric acid-hydrolyzed sample with a hexaammonium heptamolybdate reagent containing ascorbic acid. Glucose content was determined by GC.

Gas Chromatography. Fatty acid and carbohydrate composition were determined by GC using a SHIMADZU GC2014 apparatus equipped with a CBP-1 capillary column (25 m × 0.22 mm, film thickness of 0.25 mm; Shimadzu GLC, Tokyo, Japan) with increasing temperatures (from 100 to 250 °C at a rate of 5 °C/min). The sample was methanolyzed with 5% hydrogen chloride in methanol at 80 °C for 2 h. The reaction mixture was washed twice with 100 μL of hexane to extract methyl esters of fatty acids. The hexane layer was subjected to GC analysis for methyl esters of fatty acids. The methanol layer was dried by flushing with N_2 gas and then trimethylsililated with trimethylchlorosilane (TMCS) (Pierce, Rockford, IL) at 80 °C for 30 min. The trimethysililated compounds were analyzed for methyl esters of sugars.

[2] PtdGlc is completely resistant to PIPLC-mediated digestion (unpublished observation).

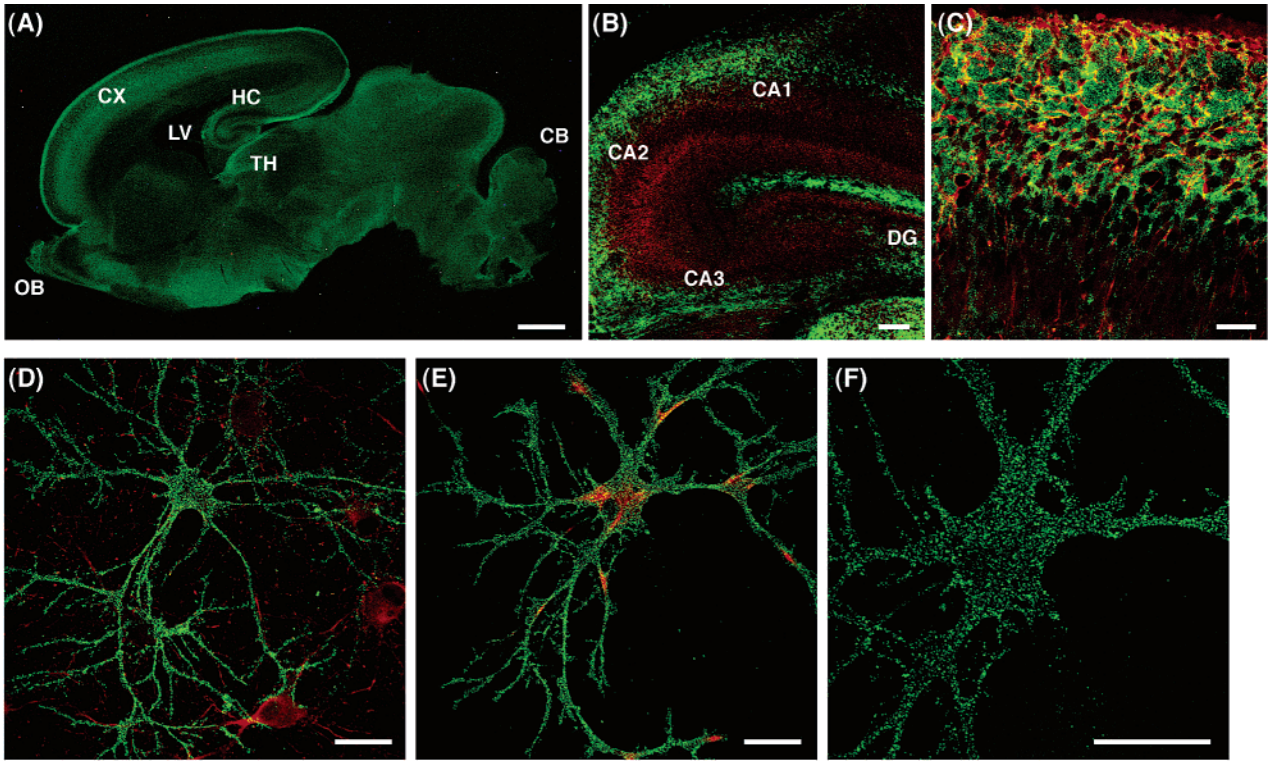

FIGURE 1: (A) E21 rat whole brain immunostained with DIM21. The scale bar is 1 mm. Abbreviations: CB, cerebellum; CX, cerebral cortex; HC, hippocampus; LV, lateral ventricle; OB, olfactory bulb; TH, thalamus. (B) Hippocampal region double immunostained with DIM21 (green) and NSE (red), as a neuronal marker. The scale bar is 100 μm. (C) Hippocampal region double immunostained with DIM21 (green) and Phgdh (red). (D) Cultured hippocampal cells double immunostained with DIM21 antigen (green) and NSE (red). Hippocampal cells were cultured for 14 days (DIV14) and then immunostained with antibodies against the DIM21 antigen and NSE. (E) Colocalization of the DIM21 antigen (green) with GFAP (red) in cultured astroglial cells at DIV14. (F) High-magnification image of the DIM21 antigen shown in panel E. The scale bar in panels C−F is 30 μm.

NMR Spectroscopy. The sample was dried thoroughly under a stream of N_2 gas, then dissolved in 200 μL of CD_3-OD, and put into a 3 mm diameter NMR microtube. The ^{1}H NMR spectra and two-dimensional total correlation spectra (TOCSY) and ^{1}H−^{31}P heteronuclear multiple-bond coherence spectra (HMBC) were measured with a JNM-ECA 600 spectrometer (JEOL Ltd., Tokyo, Japan) equipped with an HX5FG2 probe head. The operating temperature was 308 or 298 K.

Mass Spectrometry. A Bruker Daltonics (Billerica, MA) APEX-II Fourier transform mass spectrometer (FT-MS) equipped with a 7T passively shielded magnet and an in-house-fabricated nano-electrospray source (*29*) was used for the acquisition of negative ion mass spectra. The purified lipids dissolved in C:M (1:2, v/v) (modified with 10 mM ammonium acetate for stable ionization) were manually injected into a 20 μL sample loop and delivered to the nano-electrospray emitter by pumping solvent (50% methanol) at a flow rate of 200 nL/min. To accurately measure the mass of deprotonated molecules of lipids, broadband mass spectra were recorded by accumulation of 512K-point 400 kHz transient signals; the mass resolving power at *m*/*z* 893 was 46 000. For analyzing product ions from each deprotonated lipid molecule, sustained off-resonance irradiation/collision-induced dissociation (SORI-CID) (*30*) MS/MS spectra were recorded by accumulation of 1 MHz transient signals (512K points); mass resolutions at *m*/*z* 153 and 419 were 100 000 and 36 000, respectively. The *m*/*z* axes of the spectra were externally calibrated with ions attributable to sodium trifluoroacetate clusters (from separately sprayed 50% aqueous methanol) observed between *m*/*z* 112.9856 and 1064.8093 at intervals of 135.9748 units.

RESULTS AND DISCUSSION

Immunochemical Detection of PtdGlc in the Murine Central Nervous System. We identified a unique type of mammalian glycolipid, PtdGlc, through immunostaining with GL2, a human monoclonal antibody against "i" antigen, and rGL7, the recombinant Fab fragment of GL2 (*20*, *21*). For further detailed analysis of PtdGlc, we needed to develop a more specific means of identifying PtdGlc, since GL-2 and rGL-7 did not specifically react with PtdGlc. Katagiri et al. reported that immunization with the DIM fraction effectively induces the formation of mAbs against carbohydrate antigens such as SSEA-4 (*22*). This result led us to immunize mice with the DIM fraction isolated from rGL-7-stimulated HL60 cells to generate a specific mAb against PtdGlc present in the DIM fraction.

We obtained various DIM-reactive antibodies (anti-proteins and anti-lipid antibodies) and succeeded in generating DIM21, an anti-lipid mAb that preferentially recognizes membrane PtdGlc (*24*). This mAb preferentially recognized both PtdGlc isolated from HL60 cells and chemically synthesized PtdGlc (Y. Ito et al., unpublished observation).

We immunostained brain sections from E12.5 to postnatal day 21 (P21) mice with DIM21 and found that DIM21 densely stained fetal brains. The cerebral cortex from E14.5 mice, in particular, displayed strong immunoreactivity. DIM21 immunoreactivity, however, decreased greatly in the

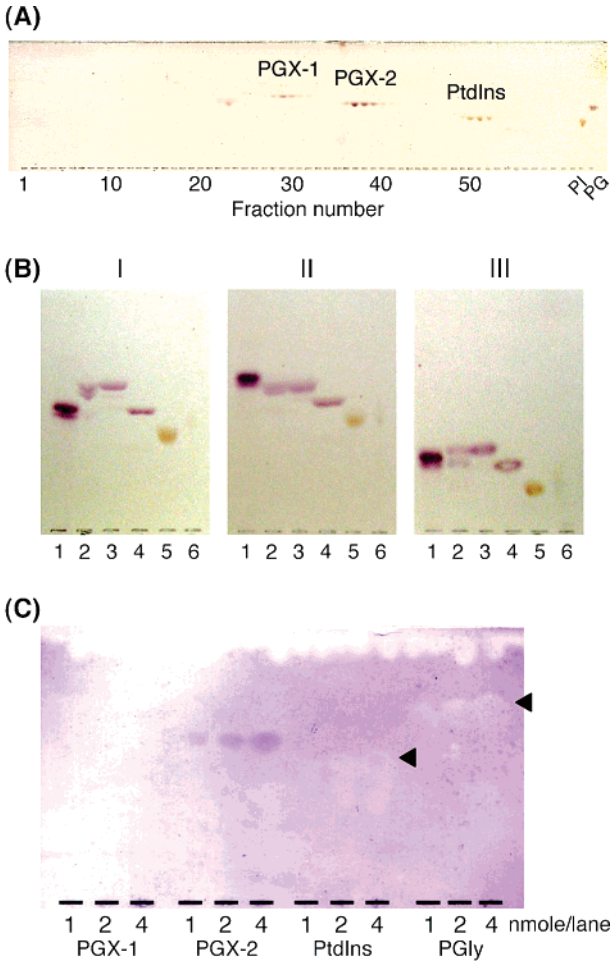

FIGURE 2: (A) TLC analysis of the final purification step of the DIM21 antigen on an Aquasil column. The immunoreactive fractions that eluted from the Q-Sepharose column were applied to a Aquasil Senshu Pack column that was part of a HPLC system (Jusco PU980). After being washed with C:M (9:1, v/v) for 10 min, the lipid sample was eluted with a gradient from 9:1 (v/v) to 7:3 (v/v) C:M for 90 min at a flow rate of 1 mL/min. The elution profile monitored by TLC with orcinol reagent is shown. The orcinol-positive, DIM-21-reactive lipids were termed PGX-1 and PGX-2 in the order they were eluted from the column. (B) TLC of PGX-1 and PGX-2: lane 1, LacCer; lane 2, sulfatide; lane 3, PGX-1; lane 4, PGX-2; lane 5, phosphatidylinositol; and lane 6, phosphatidylcholine. TLC was developed with solvent system I [C:M and 2.5 N NH_4OH (60:35:8, v/v/v)], II [C:M:W (60:35:8, v/v/v)], or III [C:acetone:M:HOAc:W (5:2:1:1:0.5, v/v/v/v/v)]. Lipids were visualized with orcinol reagent. (C) TLC immunostaining of purified glycolipids with mAb DIM21. The indicated amounts of antigens were applied to the TLC plate, which was then immunostained with mAb DIM21 as described in the text. PGly represents phosphatidylglycerol. Arrowheads indicate the position of each standard phospholipid, PtdIns and PGly.

brains of postnatal mice. At P21, DIM21 immunoreactivity was restricted to regions of active neuronal cell proliferation and differentiation. On the basis of the morphology of DIM21-immunoreactive cells and co-immunostaining with antibodies against GLAST (*31*), BLBP (*32*, *33*), and 3-phosphoglycerate dehydrogenase (Phgdh) (*34*), a key enzyme of L-serine biosynthesis, we found that cells with a radial glia/astrocyte lineage and olfactory ensheathing glia preferentially expressed DIM21 antigen. These observations suggested that DIM21 specifically recognized glial cells (M. Kinoshita et al., unpublished observation).

Table 1: Sugar and Fatty Acid Composition of PGX-1 and PGX-2

	sugar (%)		fatty acid (%)		
	glucose	others[a]	C16:0	C18::0	C20:0
PGX-1	88.0	12.0	–	48.8	51.2
PGX-2	85.3	14.7	1.0	50.0	49.0

[a] Peak area not identical to known sugars.

Because a single mouse brain contains minute PtdGlc levels, levels too low for successful isolation of pure PtdGlc, we examined DIM21 antigen expression in rat fetal brain to determine whether rat fetal brain would be a good source of PtdGlc for our structural analyses. As shown in Figure 1A, DIM21 antigen was also detectable in rat brain at E21. Interestingly, DIM21 did not immunostain neuron-specific enolase (NSE)-immunoreactive cell layers (Figure 1B) or MAP2-immunoreactive cells (data not shown). DIM21 immunoreactivity overlapped, however, with cells immunoreactive for the glial marker, Phgdh (Figure 1C).

Next, we double immunostained cultured hippocampal cells with DIM21 and either anti-NSE or anti-GFAP antibodies. NSE-immunopositive neuronal cells failed to be immunostained with DIM21 (Figure 1D). In contrast, GFAP-immunopositive astroglial cells were immunostained with DIM21, displaying scattered patches of DIM21 immunoreactivity on the cell surface (Figure 1E,F). Taken together, these findings suggest that PtdGlc localizes to the membranes of astroglial cells in the rat CNS. Control cultures immunostained in the absence of a primary antibody displayed no immunoreactivity (data not shown).

Isolation of PtdGlc from Rat Embryonic Brain. To determine the chemical structure of the DIM21 antigen in the CNS, we isolated it from lyophilized E21 fetal rat brain. The DIM21 antigen from brain was retained on phenyl boronate agarose, and during ion exchange chromatography, the DIM21 antigen was retained on Q-Sepharose equilibrated with C:M:W (30:60:8, v/v/v) and eluted by C:M and aqueous 0.1 M sodium acetate (30:60:8, v/v/v). The immunoreactive fraction retained on Q-Sepharose was collected and partitioned with Folch's system for desalting, and then the organic layer was loaded onto an Aquasil Senshu Pack column for HPLC. The elution profile of PtdGlc and related compounds retained on the Aquasil column is shown in Figure 2A. We obtained two previously unrecognized lipids that tested positively with the orcinol reaction. We termed these lipids PGX-1 and PGX-2 on the basis of the elution order from the Aquasil column.

TLC mobilities of purified PGX-1 and PGX-2 under alkaline, neutral, and acidic developmental conditions are shown in Figure 2B. Both lipids had a single spot on TLC with orcinol and molybdenum blue reagent (for phosphate), but the reactivity of PGX-1 with respect to the latter reagent was rather weak. GC analysis revealed that both PGX-1 and PGX-2 contained glucose as their sole sugar. To our surprise, both fractions contained only saturated fatty acid (C18:0 and C20:0) at an equal molar ratio (Table 1). The TLC migration of PGX-2 indicated that PGX-2 was identical to synthetic PtdGlc (data not shown).

We re-examined the binding specificity of DIM21 for PGX-1 and PGX-2 by TLC immunostaining (Figure 2C). DIM21 stained PGX-2 strongly and in a concentration-

Table 2: ^{1}H NMR Data for PGX-1 and PGX-2 in Methanol-d_4[a]

	PGX-2			PGX-1	
	major	minor		major	minor
Glc C1	4.835 dd (7.6, 7.6)	4.839 dd (7.6, 7.6)		4.859 dd (7.6, 7.6)	4.864 dd (7.6, 7.6)
Glc C2	3.22 dd (9.1, 7.6)	3.21 dd (9.1, 7.6)		3.23 dd (9.1, 7.6)	3.23 dd (9.1, 7.6)
Glc C3	3.37 dd (9.1, 9.1)	3.37 dd (9.1, 9.1)		3.39 dd (9.1, 9.1)	3.23 dd (9.1, 7.6)
Glc C4	3.27 m	3.26 m		3.32 m	3.32 m
Glc C5	3.34 m	3.34 m		3.50 m	3.50 m
Glc C6a	3.85 dd (12.1, 2.0)	3.85 dd (11.6, 2.0)		4.43 dd (12.1, 2.5)	ca. 4.43 m
Glc C6b	3.63 dd (12.1, 6.6)	3.64 dd (11.6, 6.1)		4.17 dd (12.1, 5.6)	ca. 4.17 m
Gly C1a	4.10−4.02 m	4.10−4.02 m		4.06 m	4.06 m
Gly C1b	4.10−4.02 m	4.10−4.02 m		4.00 m	4.00 m
Gly C2	5.24 m	5.24 m		5.21 m	5.21 m
Gly C3a	4.46 dd (12.1, 3.0)	4.44 dd (12.1, 3.0)		4.44 dd (12.1, 3.0)	ca. 4.44 m
Gly C3b	4.18 dd (12.1, 6.6)	4.20 dd (12.1, 7.6)		4.17 dd (12.1, 7.1)	4.20 dd (12.6, 7.6)
FA-1-$COCH_2$	2.33 t (7.2)	2.33 t (7.2)		2.32 t (7.3)	2.32 t (7.3)
FA-2-$COCH_2$	2.30 t (7.0)	2.30 t (7.0)		2.29 t (7.1)	2.29 t (7.1)
CH_2 (×2)	1.59 m	1.59 m		1.59 m	1.59 m
CH_2	1.28 m	1.28 m		1.28 m	1.28 m
Me	0.89 t (7.1)	0.89 t (7.1)		0.89 t (7.3)	0.89 t (7.3)
			6-O-Ac	2.05 s	2.05 s

[a] CD_2HOD at 3.30 ppm was used as an internal reference for ^{1}H NMR (600 MHz) at 308 K. Chemical shifts are given in parts per million, and coupling constant J values are in hertz in parentheses. Abbreviations: dd, doublet of doublets; m, multiplet; s, singlet; t, triplet.

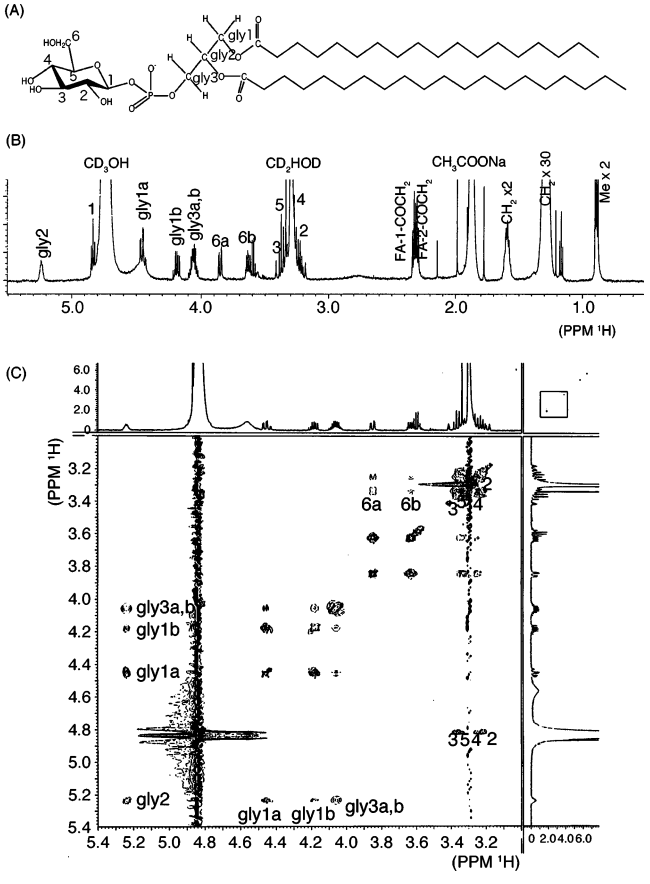

FIGURE 3: Proton NMR spectrometry of PGX-2. (A) Proposed structure of PGX-2, phosphatidyl β-D-glucoside. (B) One-dimensional proton NMR spectrum of PGX-2. (C) Two-dimensional proton−proton TOCSY spectrum of the area including glucose ring protons and glycerol protons of PGX-2.

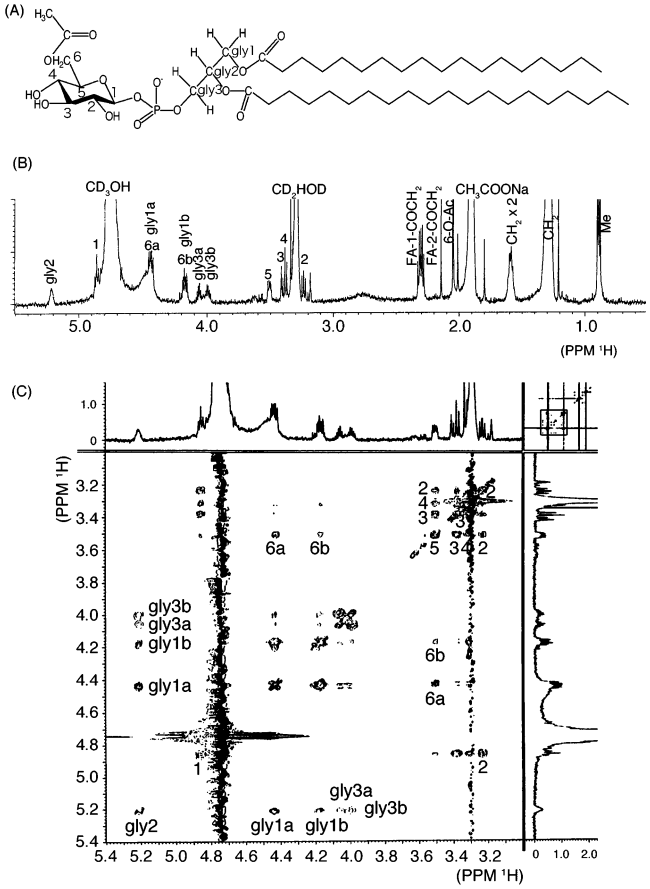

FIGURE 4: Proton NMR spectrum of PGX-1. (A) Proposed structure of PGX-1, phosphatidyl β-D-(6-*O*-acetyl)glucoside. (B) One-dimensional whole proton NMR spectrum of PGX-1. (C) Two-dimensional proton−proton TOCSY spectrum of the area including glucose ring protons and glycerol protons of PGX-1.

dependent manner, whereas DIM21 stained PGX-1 weakly. As described below, structural assessment of PGX-1 revealed that the glucose C6 position of PGX-1 is modified with an acetyl group. The TLC immunostaining results indicate that the C6 hydroxy group is critical for recognition of PtdGlc by DIM21. It is also worth mentioning that DIM21 did not show any cross reactivity with PtdIns and PGly. In our previous report (*24*), DIM21 was shown to be slightly reactive with the two lipids. Later, we found that this was due to nonspecific reaction by a second HRP-conjugated antibody. The reaction was dependent on lot number and not detectable in the HRP-labeled antibody used in the assay

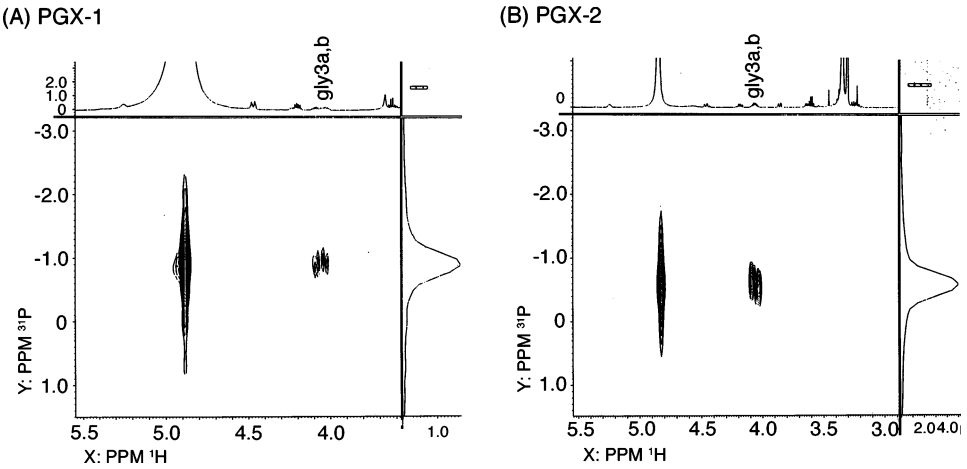

FIGURE 5: Two-dimensional $^{1}H-^{31}P$ correlation spectrum of PGX-1 (A) and PGX-2 (B).

described here. We again performed TLC immunostaining in the crude lipid extract using the new second antibody to see the specificity of DIM21. However, since the crude lipid extract contains abundant lipids such as PC, PE, PS, and PtdIns, it was impossible to separate PtdGlc from these major lipids by two-dimensional TLC and to perform immunostaining. The result of TLC immunostaining in the acidic lipid fraction from Q-Sepharose column chromatography showed that lipids such as PtdIns and the other acidic lipids were not reactive with DIM21 and PtdGlc was only an active lipid (data not shown).

Structural Analysis of PGX-2 by 600 MHz NMR Spectrometry. A major DIM21-immunoreactive glycolipid, PGX-2, was subjected to proton NMR analysis (Figure 3). PGX-2 contained a β-glucose anomeric proton with a chemical shift of 4.835 ppm and J_1 and J_2 values of 7.6 and 7.6 Hz, respectively. The anomeric signal split into three peaks, indicating the presence of the Glc (1β-phosphate) structure in PGX-2 (*35*).

Two-dimensional $^{1}H-^{1}H$ TOCSY spectra demonstrated that the glucose ring of PGX-2 has a complete assignment of protons (Figure 3C and Table 2). One-dimensional ^{1}H signals were attributed to Glc C2 (δ_H 3.22 ppm, $J_{1,2}$ dd 9.1 and 7.6 Hz), Glc C3 (δ_H 3.37 ppm, $J_{1,2}$ dd 9.1 and 9.1 Hz), Glc C4 (δ_H 3.27 ppm, m), Glc C5 (δ_H 3.34 ppm, m), Glc C6a (δ_H 3.85 ppm, $J_{1,2}$ dd 12.1 and 2.0 Hz), and Glc C6b (δ_H 3.63 ppm, $J_{1,2}$ dd 12.1 and 6.6 Hz). The glycerol moiety was also shown to contain glycerol C1a (δ_H 4.46 ppm, $J_{1,2}$ dd 12.1 and 4.0 Hz), glycerol C1b (δ_H 4.18 ppm, $J_{1,2}$ dd 12.1 and 6.6 Hz), glycerol C2 (δ_H 5.24 ppm, m), and glycerol C3 (δ_H 4.10−4.12 ppm, m). The presence of a correlation between glucose C1 and glycerol C3 and ^{31}P confirmed the presence of a Glcβ1−phosphate−glycerol C3 structure in the PGX-2 molecule (Figure 5B).

Notably, additional minor signals at the glucose 1 and glycerol 1a,b peaks were detectable in the enlarged one-dimensional ^{1}H spectrum (Figure 6A and Table 2). The chemical shifts and coupling constants (^{3}J) were assessed by two-dimensional $^{1}H-^{1}H$ TOCSY spectra (Table 2), which suggested that the minor component was a stereoisomer of PtdGlc. In comparison with the two synthetic stereoisomers of PtdGlc, C1 of the minor component was confirmed to have a phosphate group and not a hydroxy group (Y. Ito et al., unpublished data). Thus, PGX-2 purified from rat

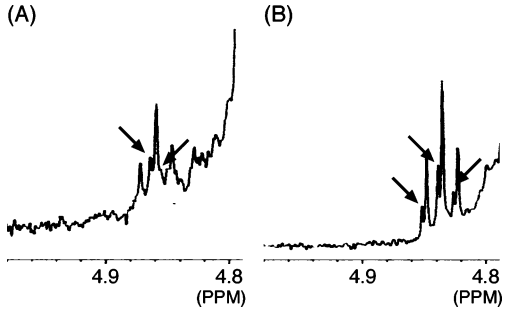

FIGURE 6: Minor peaks of NMR spectra. Parts of the NMR spectra of PGX-1 (A) and PGX-2 (B) were extracted and enlarged. Arrows denote minor peaks.

embryonic brain was a mixture of two stereoisomers: 3-*sn*-phosphatidylglucoside (~85%) and 1-*sn*-phosphatidylglucoside (~15%). How 1-*sn*-phosphatidylgucoside is synthesized in cells is an interesting issue that remains to be elucidated.

Structural Analysis of PGX-1 by 600 MHz NMR Spectrometry. PGX-1 was subjected to one- and two-dimensional ^{1}H NMR analysis (Figure 4). Assignment of each signal is summarized in Table 2.

NMR showed that PGX-1 was analogous to PGX-2. The chemical shifts of the β-glucose anomeric proton at 4.859 ppm ($J_{1,2}$ 7.6 and 7.6 Hz) of PGX-1 were essentially similar to those of PGX-2 (PtdGlc). The major anomeric signal also split into three peaks, indicating the presence of a Glc with a β1-phosphate linkage in PGX-1.

The complete assignment of glucose ring protons was confirmed by ^{1}H TOCSY spectra (Figure 4B): Glc C2 (δ_H 3.23 ppm, $J_{1,2}$ dd 9.1 and 7.6 Hz), Glc C3 (δ_H 3.39 ppm, $J_{1,2}$ dd 9.1 and 9.1 Hz), Glc C4 (δ_H 3.32 ppm, m), Glc C5 (δ_H 3.50 ppm, m), Glc C6a (δ_H 4.43 ppm, $J_{1,2}$ dd 12.1 and 2.5 Hz), and Glc C6b (δ_H 4.17 ppm, $J_{1,2}$ dd 12.1 and 5.6 Hz). Compared to the Glc C6 proton of PGX-2, the Glc C6 proton of PGX-1 shifted significantly to a lower field (Figures 3B,C and 4B,C and Table 2), suggesting a substitution at the C6 position of glucose.

The glycerol moiety was identified as glycerol C1a (δ_H 4.06 ppm, m), glycerol C1b (δ_H 4.00 ppm, m), glycerol C2 (δ_H 5.21 ppm, m), glycerol C3a (δ_H 4.44 ppm, $J_{1,2}$ dd 12.1 and 3.0 Hz), and glycerol C3b (δ_H 4.17 ppm, $J_{1,2}$ dd 12.1 and 7.1 Hz). The presence of a correlation between both

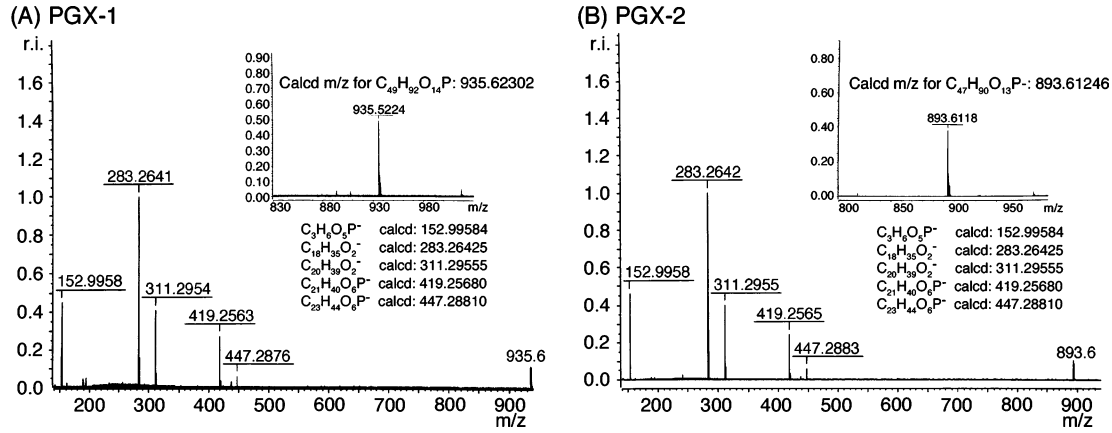

FIGURE 7: FT-ICR mass spectrometry of PGX-1 (A) and PGX-2 (B). (A) SORI-CID product ion spectrum of a deprotonated molecule of PGX-1, *m/z* 935.6. Assignments of product ions shown in panel A: 447.2876, $C_{23}H_{44}O_6P^-$ (formal loss of stearoyl and acetyl glucoside); 419.2563, $C_{21}H_{40}O_6P$ (formal loss of arachidoyl and acetyl glucoside); 311.2954, $C_{20}H_{39}O_2^-$ (arachidate anion); 283.2641, $C_{18}H_{35}O_2^-$ (stearate anion); and 152.9958, $C_3H_6O_5P^-$ (formally, 3-hydroxy-1,2-propylene phosphate anion). Deprotonated molecule of PGX-1 at *m/z* 935.6224 (observed in the regular mass spectrum without SORI-CID), with $C_{49}H_{92}O_{14}P^-$ shown in the inset. (B) Product ion spectrum from PGX-2 with an ion at *m/z* 893.6. Assignments of product ions shown in panel B: 447.2883, $C_{23}H_{44}O_6P^-$ (formal loss of stearoyl and acetyl glucoside); 419.2565, $C_{21}H_{40}O_6P$; 311.2955, $C_{20}H_{39}O_2^-$; 283.2642, $C_{18}H_{35}O_2^-$; and 152.9958, $C_3H_6O_5P^-$. Deprotonated molecule of PGX-2 at *m/z* 893.6118 (in the regular mass spectrum), with $C_{47}H_{90}O_{13}P^-$ shown in the inset. The difference between observed masses for deprotonated molecules of PGX-1 (935.6224) and PGX-2 (893.6118) is 41.0106, corresponding to substitution of a hydrogen for an acetyl group, C_2H_2O (calculated mass of 41.01056).

glucose C1 and glycerol C3 and ^{31}P confirmed the presence of a Glc−1-phosphate−glycerol C3 structure in the PGX-1 molecule (Figure 5A).

Additional minor signals at the glucose 1, glucose 3, and glycerol 3b peaks were detectable (Figure 6A and Table 2). As in PGX-2, these signals were supposedly derived from a stereoisomer of PGX-1. The major component had a glucose 1-phosphate at the *sn*-3 position, while the minor component had a glucose 1-phosphate at the *sn*-1 position.

Analysis of PGX-1 and PGX-2 by Mass Spectrometry. PGX-1 and PGX-2 were subjected to MS analysis to ascertain their exact molecular masses and to identify the substituted group in PGX-1. Negative ion FT-ICR-MS detected the deprotonated molecule of PGX-2 at *m/z* 893.6118 (Figure 7B, inset), which corresponded to the calculated monoisotopic mass of 893.61246 for $C_{47}H_{90}O_{13}P^-$, a phosphatidylglucoside containing stearic acid (C18:0) and arachidic acid (C20:0). A single major peak appeared in the mass spectrum, indicating the homogeneity of the phosphatidic acid moiety of the phosphatidylglucoside from fetal rat brain.

The deprotonated molecule of PGX-1 was detected at *m/z* 935.6224 (Figure 7A, inset). This value corresponds to the calculated monoisotopic mass of 935.62302 for $C_{49}H_{92}O_{24}P^-$, indicating that PGX-1 was a modified form of PGX-2 that contained an acetate group. Since the glucose C6 proton signals of PGX-1 shifted to a lower magnetic field on NMR analysis (Figure 5) compared to those of PGX-2, PGX-1 was determined to be phosphatidyl β-D-(6-*O*-acetyl)glucoside.

MS/MS analysis indicated that the product ion spectra of both PGX-1 and PGX-2 were almost identical (Figure 7).

Finally, we determined the position of each fatty acyl chain in the glycerol backbone of PGX-1 and PGX-2. Both lipids were sensitive to bee venom phospholipase A2. GC analysis revealed that the remaining fatty acid in lyso-PtdGlc was stearic acid. Thus, stearic aid and arachidic acid are attached to the C1 and C2 positions, respectively, of the phosphatidyl group. Taken together, these findings indicate that the main glucose-containing phosphoglycerolipids isolated from fetal rat brain were 1-stearyl-2-arachidoyl-*sn*-glycerol-3-phosphoryl β-D-glucopyranoside (PGX-2) and 1-stearyl-2-arachidoyl-*sn*-glycerol-3-phosphoryl β-D-(6-*O*-acetyl)glucopyranoside (PGX-1) (Figures 3 and 4).

This is the first report to prove that PtdGlc exists in mammalian tissues. Since the mass numbers of glycolipids are the same as that of PtdIns, PtdGlc has been difficult to identify solely by conventional mass spectrometric analysis. This may be the main reason PtdGlc has been overlooked until now. It is important to note that the presence of acetylated PtdGlc was not an artifact during the purification. Just recently, we have established a method of identifying PtdGlc and acetylated PtdGlc by HPLC/MS/MS (electrospray ionization ion-trap mass spectrometry). By this method, we can discriminate PtdGlc from PI because the elution time from HPLC and the fragmentation pattern of MS/MS are different (unpublished results). This analytical data proved that acetylated PtdGlc as well as PtdGlc is present even in crude lipid extracts (chloroform/methanol extracts) from fetal rodent brains and HL60 cells. Thus, we can exclude the possibility that the PtdGlc was acetylated during the purification or that acetyl-PtdGlc was deacetylated during the purification.

Unexpectedly, we found that fetal rat brain PtdGlc is composed exclusively of saturated fatty acids (stearic and arachidic acids). The presence of arachidic acid, in particular, in glycerolipids has been described very little. This fatty acid composition may explain why PtdGlc is enriched in the DIM fraction, as is GSL.[3] Brown and London (*2*, *36*) suggested that the highly ordered solidlike gel phase of lipids composed of GSL and cholesterol in membranes was essential for the detergent insolubility of the raftlike membrane domain. By comparing the GM95 GSL-deficient mutant cell line with

[3] DSC (differential scanning calorimetry) analysis showed that PtdGlc has a high melting temperature comparable to that of GSLs (T. Kobayashi, unpublished observation).

wild type melanoma cells, Ostermeyer et al. (*37*) concluded that GSLs were not essential for formation of lipid rafts. A more recent study showed that all classical glycerophospholipids exist in lipid rafts isolated from the Jurkatt T cell line and that these glycerophospholipids are involved in TCR signaling (*38*). Sandhoff et al. reported that glucosylceramide in lipid rafts isolated from testicular tissue contained very long chains of polyunsaturated fatty acid residues (e.g., 28:5 and 30:5) in their ceramide moieties and that these long chains played a role in spermatogenesis (*39*). These results strongly suggest that structural analysis of lipid rafts, including fatty acyl moieties, is important for understanding the physiological function and localization of lipid molecules in rafts.

It is very important to know what the active lipid for DIM21 in the biological membranes is. To address this question, we have to wait until we have the gene involved in PtdGlc synthesis or isolate an enzyme to destroy membrane PtdGlc specifically. At present, all we can tell is that the hydrophobic chain of PtdGlc may be a critical part for presentation of glucose (phosphate) essential for DIM21 recognition. PtdGlc contains exclusively 18:0/20:0 fatty acyl chains. The saturated fatty acyl chains may give a unique property to the biological membranes; in our preliminary experiment, we found that PtdGlc forms clusters or aggregates in model membranes (T. Kobayashi et al., unpublished results). We speculate that the aggregated form of PtdGlc may be present in vivo and the aggregated lipid (high-density form) can more easily be recognized by the IgM type monoclonal antibody of DIM21.

As shown in Figure 1F, DIM21 immunostained the surface of glial cells in a dotlike fashion. Depleting cell membranes of cholesterol with 10 mM methyl-β-cyclodextrin (data not shown) abolished this punctate staining pattern, indicating that PtdGlc resides within distinct membrane microdomains, i.e., rafts, on astroglial cells. At present, the biological roles of PtdGlc in glial cells remain unknown and need to be elucidated. We believe, however, that the characteristic presence of an arachidic acid fatty acyl chain suggests that PtdGlc may play an important role in glial cell development and differentiation. Analyzing the physicochemical properties of PtdGlc may help us understand its roles in lipid rafts or microdomain formation and organization.[3]

Since arachidic acid is rarely found in mammalian lipids, PtdGlc is presumably biosynthesized by a pathway different from those that synthesize known phospholipids. Thus, determining how PtdGlc is synthesized in glial cells would also be important.

ACKNOWLEDGMENT

We thank Drs. Peter Greimel and Yukishige Ito (RIKEN) for providing synthetic PtdGlc and its stereoisomer. We are grateful to Dr. Toshihide Kobayashi (RIKEN) for helpful discussions.

REFERENCES

1. Simons, K., and Ikonen, E. (1997) Functional rafts in cell membranes, *Nature 387*, 569−572.
2. Brown, D. A., and London, E. (2000) Structure and function of sphingolipid- and cholesterol-rich membrane rafts, *J. Biol. Chem. 275*, 17221−17224.
3. Brown, D. A., and London, E. (1998) Function of lipid rafts in biological membranes, *Annu. Rev. Cell Dev. Biol. 14*, 111−136.
4. Simons, K., and Ikonen, E. (2000) How cells handle cholesterol, *Science 290*, 1722−1726.
5. Hakomori, S.-I. (2002) The glycosynapse, *Proc. Natl. Acad. Sci. U.S.A. 99*, 225−232.
6. Takenouchi, H., Kiyokawa, N., Taguchi, T., Matsui, J., Katagiri, Y. U., Okita, H., Okuda, K., and Fujimoto, J. (2004) Shiga toxin binding to globotriaosyl ceramide induces intracellular signals that mediate cytoskeleton remodeling in human renal carcinoma-derived cells, *J. Cell Sci. 117*, 3911−3922.
7. Nagahama, M., Yamaguchi, A., Hagiyama, T., Ohkubo, N., Kobayashi, K., and Sakurai, J. (2004) Binding and internalization of *Clostridium perfringens* iota-toxin in lipid rafts, *Infect. Immun. 72*, 3267−3275.
8. Shima, T., Nada, S., and Okada, M. (2003) Transmembrane phosphoprotein Cbp senses cell adhesion signaling mediated by Src family kinase in lipid rafts, *Proc. Natl. Acad. Sci. U.S.A. 100*, 14897−14902.
9. Herincs, Z., Corset, V., Cahuzac, N., Furne, C., Castellani, V., Hueber, A. O., and Mehlen, P. (2005) DCC association with lipid rafts is required for netrin-1-mediated axon guidance, *J. Cell Sci. 118*, 1687−1692.
10. Falk, J., Thoumine, O., Dequidt, C., Choquet, D., and Faivre-Sarrailh, C. (2004) NrCAM Coupling to the Cytoskeleton Depends on Multiple Protein Domains and Partitioning into Lipid Rafts, *Mol. Biol. Cell 15*, 4695−4709.
11. Hakomori, S.-I., and Igarashi, Y. (1995) Functional role of glycosphingolipids in cell recognition and signaling, *J. Biochem. 118*, 1091−1103.
12. Toledo, M. S., Suzuki, E., Handa, K., and Hakomori, S.-I. (2004) Cell growth regulation through GM3-enriched microdomain (glycosynapse) in human lung embryonal fibroblast WI38 and its oncogenic transformant VA13, *J. Biol. Chem. 279*, 34655−34664.
13. Kasahara, K., and Sanai, Y. (2000) Functional roles of glycosphingolipids in signal transduction via lipid rafts, *Glycoconjugate J. 17*, 153−162.
14. Pike, L. (2003) Lipid rafts: Bringing order to chaos, *J. Lipid Res. 44*, 655−667.
15. Mukherjee, A., Arnaud, L., and Cooper, J. A. (2003) Lipid-dependent recruitment of neuronal Src to lipid rafts in the brain, *J. Biol. Chem. 278*, 40806−40814.
16. Guirland, C., Suzuki, S., Kojima, M., Lu, B., and Zheng, J. Q. (2004) Lipid rafts mediate chemotropic guidance of nerve growth cones, *Neuron 42*, 51−62.
17. Schaeren-Wiemers, N., Bonnet, A., Erb, M., Erne, B., Bartsch, U., Kern, F., Mantei, N., Sherman, D., and Suter, U. (2004) The raft-associated protein MAL is required for maintenance of proper axon−glia interactions in the central nervous system, *J. Cell Biol. 166*, 731−742.
18. Vinson, M., Rausch, O., Maycox, P. R., Prinjha, R. K., Chapman, D., Morrow, R., Harper, A. J., Dingwall, C., Walsh, F. S., Burbidge, S. A., and Riddell, D. R. (2003) Lipid rafts mediate the interaction between myelin-associated glycoprotein (MAG) on myelin and MAG-receptors on neurons, *Mol. Cell. Neurosci. 22*, 344−352.
19. Gellermann, G. P., Appel, T. R., Tannert, A., Radestock, A., Hortschansky, P., Schroeckh, V., Leisner, C., Lutkepohl, T., Shtrasburg, S., Rocken, C., Pras, M., Linke, R. P., Diekmann, S., and Fandrich, M. (2005) Raft lipids as common components of human extracellular amyloid fibrils, *Proc. Natl. Acad. Sci. U.S.A. 102*, 6297−6302.
20. Nagatsuka, Y., Kasama, T., Uzawa, J., Ohashi, Y., Ono, Y., and Hirabayashi, Y. (2001) A new phosphoglycerolipid, "phosphatidyl glucose", found in human cord red cells by multi-reactive monoclonal anti-i cold agglutinin, mAb GL-1/GL-2, *FEBS Lett. 497*, 141−147.
21. Nagatsuka, Y., Hara-Yokoyama, M., Kasama, T., Takekoshi, M., Maeda, F., Ihara, S., Fujiwara, S., Ohshima, E., Ishii, K., Kobayashi, T., Shimizu, K., and Hirabayashi, Y. (2003) Carbohydrate-dependent signaling from the phosphatidyl glucoside based microdomain induces differentiation of HL60 cells, *Proc. Natl. Acad. Sci. U.S.A. 100*, 7454−7459.
22. Katagiri, Y. U., Ohmi, K., Katagiri, C., Sekino, T., Nakajima, H., Ebata, T., Kiyokawa, N., and Fujimoto, J. (2001) Prominent immunogenicity of monosialosyl galactosylgloboside, carrying a stage-specific embryonic antigen-4 (SSEA-4) epitope in the ACHN human renal tubular cell line: A simple method for producing

monoclonal antibodies against detergent-insoluble microdomains/raft, *Glycoconjugate J. 18*, 347−353.
23. Katagiri, Y. U., Ohmi, K., Tang, W., Takenouchi, H., Taguchi, T., Kiyokawa, N., and Fujimoto, J. (2002) Raft.1, a monoclonal antibody raised against the raft microdomain, recognizes G-protein β1 and 2, which assemble near nucleus after shiga toxin binding to human renal cell line, *Lab. Invest. 82*, 1735−1745.
24. Yamazaki, Y., Nagatsuka, Y., Oshima, E., Suzuki, Y., Hirabayashi, Y., and Hashikawa, T. (2006) Comprehensive analysis of monoclonal antibodies against detergent-insoluble membrane/lipid rafts from HL60 cells, *J. Immunol. Methods 311*, 106−116.
25. Mitoma, J., Kasama, T., Furuya, S., and Hirabayashi, Y. (1998) Occurrence of an unusual phospholipid, phosphatidyl-L-threonine, in cultured hippocampal neurons exogeneous L-serine is required for the synthesis of neuronal phosphatidyl-L-serine and sphingolipids, *J. Biol. Chem. 273*, 19363−19366.
26. Ikezawa, H., Yamanegi, M., Taguchi, R., Miyashita, T., and Ohyabu, T. (1976) Studies on phosphatidylinositol phosphodiesterase (phospholipase C type) of *Bacillus cereus*. I. purification, properties and phosphatase-releasing activity, *Biochim. Biophys. Acta 450*, 154−164.
27. Higashi, H., Hirabayashi, Y., Fukui, Y., Naiki, M., Matsumoto, M., Ueda, S., and Kato, S. (1985) Characterization of N-glycolylneuraminic acid-containing gangliosides as tumor-associated Hanganutziu-Deicher antigen in human colon cancer, *Cancer Res. 45*, 3796−3802.
28. Higashi, H., Fukui, Y., Ueda, S., Kato, S., Hirabayashi, Y., Matsumoto, M., and Naiki, M. (1984) Characterization of N-glycolyneuraminic acid-containing glycosphingolipids from a Marek's disease lymphoma-derived chicken cell line, MSB1, as tumor-associated heterophile Hanganutziu-Deicher antigens, *J. Biochem. 95*, 785−794.
29. Nakamura, T., Dohmae, N., and Takio, K. (2004) Characterization of a digested protein complex with quantitative aspects: An approach based on accurate mass chromatographic analysis with Fourier transform-ion cyclotron resonance mass spectrometry, *Proteomics 4*, 2558−2566.
30. Gauthier, J. W., Trautman, T. R., and Jacobson, D. B. (1991) Sustained off-resonance irradiation for collision-activated dissociation involving Fourier transform mass spectrometry. Collision-activated dissociation technique that emulates infrared multiphoton dissociation, *Anal. Chim. Acta 246*, 211−225.
31. Shibata, T., Yamada, K., Watanabe, M., Ikenaka, K., Wada, K., Tanaka, K., and Inoue, Y. (1997) Glutamate transporter GLAST is expressed in the radial glia-astrocyte lineage of developing mouse spinal cord, *J. Neurosci. 17*, 9212−9219.
32. Feng, L., and Heintz, N. (1995) Differentiating neurons activate transcription of the brain lipid-binding protein gene in radial glia through a novel regulatory element, *Development 121*, 1719−1730.
33. Feng, L., Hatten, M. E., and Heintz, N. (1994) Brain lipid-binding protein (BLBP): A novel signaling system in the developing mammalian CNS, *Neuron 12*, 895−908.
34. Yamasaki, M., Yamada, K., Furuya, S., Mitoma, J., Hirabayashi, Y., and Watanabe, M. (2001) 3-Phosphoglycerate dehydrogenase, a key enzyme for L-serine biosynthesis, is preferentially expressed in the radial glia/astrocyte lineage and olfactory ensheathing glia in the mouse brain, *J. Neurosci. 21*, 7691−7704.
35. Schmidt, R. R., Stumpp, M., and Michel, J. (1982) α- and β-D-glucopyranosyl phosphate from 0-α-D-glucopyranosyl trochloroacetimidates, *Tetrahedron Lett. 23*, 405−408.
36. Brown, D. A., and London, E. (1998) Structure and origin of ordered lipid domains in biological membranes, *J. Membr. Biol. 164*, 103−114.
37. Ostermeyer, A. G., Beckrich, B. T., Iverson, K. A., Grove, K. E., and Brown, D. A. (1999) Glycosphingolipids are not essential for formation of detergent-resistant membrane rafts in melanoma cells, *J. Biol. Chem. 274*, 34459−34466.
38. Rouquette-Jazdanian, A. K., Pelassy, C., Breittmayer, J. P., Cousin, J. L., and Aussel, C. (2002) Metabolic labelling of membrane microdomains/rafts in Jurkat cells indicates the presence of glycerophospholipids implicated in signal transduction by the CD3 T-cell receptor, *Biochem. J. 363*, 645−655.
39. Sandhoff, R., Geyer, R., Jennemann, R., Paret, C., Kiss, E., Yamashita, T., Gorgas, K., Sijmonsma, T. P., Iwamori, M., Finaz, C., Proia, R. L., Wiegandt, H., and Groene, H. J. (2005) Novel class of glycosphingolipids involved in male fertility, *J. Biol. Chem. 280*, 27310−27318.

BI0606546